Available online at www.sciencedirect.com
ScienceDirect
Biochemical and Biophysical Research Communications 361 (2007) 68–73
BBRC
www.elsevier.com/locate/ybbrc

Artificial neural networks and decision tree model analysis of liver cancer proteomes

John M. Luk [a,*], Brian Y. Lam [a,1], Nikki P.Y. Lee [a], David W. Ho [a], Pak C. Sham [b], Lei Chen [a,c], Jirun Peng [c], Xisheng Leng [c], Philip J. Day [d], Sheung-Tat Fan [a]

[a] *Department of Surgery and Center for Cancer Research, Faculty of Medicine Building, 9/F, 21 Sassoon Road, University of Hong Kong, Pokfulam, Hong Kong*
[b] *Genome Research Centre and Department of Psychiatry, University of Hong Kong, Pokfulam, Hong Kong*
[c] *Department of Surgery, People's Hospital, Peking University, Beijing, China*
[d] *The Manchester Interdisciplinary Biocentre, University of Manchester, Manchester, UK*

Received 25 June 2007
Available online 10 July 2007

Abstract

Hepatocellular carcinoma (HCC) is a heterogeneous cancer and usually diagnosed at late advanced tumor stages of high lethality. The present study attempted to obtain a proteome-wide analysis of HCC in comparison with adjacent non-tumor liver tissues, in order to facilitate biomarkers' discovery and to investigate the mechanisms of HCC development. A cohort of 66 Chinese patients with HCC was included for proteomic profiling study by two-dimensional gel electrophoresis (2-DE) analysis. Artificial neural network (ANN) and decision tree (CART) data-mining methods were employed to analyze the profiling data and to delineate significant patterns and trends for discriminating HCC from non-malignant liver tissues. Protein markers were identified by tandem MS/MS. A total of 132 proteome datasets were generated by 2-DE expression profiling analysis, and each with 230 consolidated protein expression intensities. Both the data-mining algorithms successfully distinguished the HCC phenotype from other non-malignant liver samples. The detection sensitivity and specificity of ANN were 96.97% and 87.88%, while those of CART were 81.82% and 78.79%, respectively. The three biological classifiers in the CART model were identified as cytochrome b5, heat shock 70 kDa protein 8 isoform 2, and cathepsin B. The 2-DE-based proteomic profiling approach combined with the ANN or CART algorithm yielded satisfactory performance on identifying HCC and revealed potential candidate cancer biomarkers.

Keywords: Cancer proteome; Classification; CART; ANN; Hepatocellular carcinoma

Liver cancer is one of the most life-threatening solid tumors, with global annual diagnosis exceeding one million new cases, and remains the second leading cause of cancer death in China. Major risk factors of HCC include chronic hepatitis virus infections, in particular hepatitis B and hepatitis C; cirrhosis caused by either hepatitis or alcoholism [1], and chronic exposures to various cytotoxic substances such as arsenic [2], polyvinyl chloride (PVC) [3], etc. The diagnosis of liver cancer usually occurs at later stages in the disease when there are few effective treatment options and the prognosis for patients with HCC is very poor. Currently, surgery remains the standard treatment for HCC patients; nevertheless, more than half of the subjects are often inoperable at the time of presentation. In addition, tumor recurrence is commonplace (>60%) after resection with vastly shortened life expectancy of about 6 months from the time of diagnosis [4,5]. In order to pursue a better disease management of liver cancer, there is an urgent need to develop models for early cancer detection, and better understand the fundamental mechanisms leading to HCC development. Proteomic expression profiling approaches

* Corresponding author. Fax: +852 2819 9636.
E-mail address: jmluk@hkucc.hku.hk (J.M. Luk).
[1] Present address: Department of Pharmacology, University of Cambridge, Cambridge, UK.

0006-291X/$ - see front matter © 2007 Elsevier Inc. All rights reserved.
doi:10.1016/j.bbrc.2007.06.172

have recently gained momentum in deciphering holistic protein expression patterns in a variety of cancer biomarker discovery studies, and similarly would unravel the biologically significant patterns, or fingerprints associated with the changes and development of liver cancer.

Recent proteomic efforts have largely focused on cultured cancer cell lines, tumor tissues as well as blood samples from HCC patients utilizing the gel-based and protein-chip approaches [6–13]. Nevertheless, neither a liver cancer specific pattern, nor a reliable classification model has been established for the diagnosis of HCC. In this study, we employed 2-DE to generate protein expression profiles of 66 tumor and 66 non-tumor paired samples, and two different data-mining engines to construct classification models with attempts to distinguish HCC from non-tumor liver tissues—artificial neural network (ANN) [14] and classification and regression tree (CART) [15,16] algorithms. The discriminative performance of the two models was compared and evaluated, and the protein classifiers were unequivocally identified by tandem MS/MS.

Materials and methods

Clinical tissues and 2-DE analysis. A total of 132 tumor and non-tumor tissues were collected from 66 patients who had undergone hepatectomy at Queen Mary Hospital, Hong Kong, from 1998 to 2004. The clinicopathological features are summarized in Table 1. Proteins were extracted from samples using the Bio-Rad ReadyPrep Sequential Extraction Kit (Bio-Rad Laboratories, Hercules, CA), and were then subjected to 2-DE using IPGphor and EttanDALT six system (Amersham Biosciences/GE Healthcare, Uppsala, Sweden) as previously described [17,18]. The gel images were acquired and analyzed using a PD-Quest version 7.2 (Bio-Rad). The intensity of each spot was normalized to the total spot intensities on gel, and the protein abundance was reported as parts per million (ppm). Preliminary examination of the data revealed 230 consistently expressed proteins with at least 70% presence in either tumor or non-tumor samples, and 92 proteins showed changes in expression level with statistical significance of $p < 0.05$. The proteome dataset was randomly divided into training and simulation sets with each set consisting of 33 tumor and 33 non-tumor samples (i.e., a total of $66 + 66 = 132$ samples). The data in the training dataset were used for training the network while the simulation dataset was used for evaluation of the classification models.

Table 1
Clinicopathological features of samples used in this study

Clinicopathological parameters	Frequencies
Sex	
Female	9
Male	57
Age[a]	53.95 ± 1.55
HBV surface antigen	
Positive	57
Negative	9
Serum alpha-fetoprotein level	
$\leqslant$20 ng/ml	20
>20 ng/ml	46
Tumor size (cm)[a]	8.80 ± 0.66
AJCC tumor stage	
Stage I/II	41
Stage III/IV	25
Non-tumorous liver	
Chronic hepatitis	8
Cirrhotic	26
Non-cirrhotic	32

[a] Values are shown as means ± SEM.

In-gel digestion and mass spectrometry (MS). Protein spots of interest were gel-excised using a syringe needle and subjected to in-gel trypsin digestion as previously described [17]. The resulting tryptic digested peptides were analyzed using MALDI-TOF/MS and MS/MS. For MALDI-TOF/MS for SSP0026 and SSP3102, full scan and product ion mass spectra of the peptide mixtures were acquired on a hybrid quadrupole-time of flight mass spectrometer (QSTAR-XL, Applied Biosystems Inc., Foster City, CA, USA), equipped with a MALDI source. The tandem mass spectra were collected in product ion mode on the peptide of interest. Measured peptide and fragment ion masses were used to search the NCBI database for protein identifications using the Mascot (www.matrixscience.com), with the following settings: mass tolerance at 50 ppm, one missed cleavage allowed, at least two matching peptides and searches limited to *Homo sapiens* species. For SSP2201, tandem MS/MS was performed using a 4800 MALDI TOF/TOF Analyzer (Applied Biosystems). In brief, MS spectra were acquired for each protein spot with the following settings: MS reflector positive and scan range of 1000–4000 Da. The resulting data were used to generate a peak list for the subsequent result dependent acquisition (RDA). Intense peaks for up to 20 peaks were subjected to MS/MS analysis for determining the peptide sequence. The MS/MS settings used were MS/MS 2KV positive/CID on and five monoisotopic precursors selected ($S/N > 200$). Tryptic peptides were excluded in the sample. Full reports with detailed Mascot results were generated in PDF format using the GPS Explorer Software (MASCOT Database Search Engine V2.1, Applied Biosystems). A high confidence protein with at least two peptide matches was recognized when the CI of the protein score and total ion exceeded 95%.

Artificial neural network (ANN). For the ANN implementation, the feed-forward multiple layer perceptron based classification model was implemented using neural network toolbox bundled in MATLAB 7.0 Release 14 (The Mathworks Inc., Natick, MA). The proteomic data were first reduced by filtering spots without significant changes between tumor and non-tumor ($p \geqslant 0.05$), then the spot intensities were natural log-transformed followed by normalization using the min–max values of the dataset. The best ANN constructed in this study consisted of 92 inputs, 2 hidden and 1 output layers with linear output ranged from -1 to 1 corresponding to tumor and non-tumor, respectively (Fig. 1). The training of the network was carried out using Leven–Marquardt back-propagation algorithm and the mean square error performance goal was 1×10^{-30}.

Classification and regression tree (CART). CART was implemented using Biomarker Pattern Software (BPS) Version 4.0 (Ciphergen Biosystems Inc., Fremont, CA). Unlike clustering and ANN, all the spots in the dataset were natural log-transformed and used for training. The classification model was constructed using GINI impurity criterion for splitting and estimation was performed using 10-fold cross-validation.

Statistical analysis. Sample size was estimated and calculated using Statmate program for Windows (GraphPad Software, Inc., San Diego, CA). After pilot experiments, a standard deviation of 573 ppm for the protein spot SSPP8103 from tumor tissues with an intensity of 311 ppm was entered into the program with a p value of 0.05. A sample size of about 60 was used when 90% power was used to detect a statistically significant difference of 357 in intensity of protein spots between tumor and non-tumor samples. SPSS for Windows (version 13, SPSS, Inc., Chicago, IL) was used for statistical and correlation analysis in this study. One-way ANOVA followed by Tukey or Dunnett's T3 test, Student's t test, and Pearson Chi-Square test were used to analyze spot intensities among peri-tumor and tumor samples. The discrimination performance was evaluated by plotting the receiver operating characteristic (ROC) curve and calculating the area under the ROC curve (AUROC). $p < 0.05$ was considered as statistically significant. Sensitivity and specificity were defined as the proportion of true positives (tumor) of all positive samples

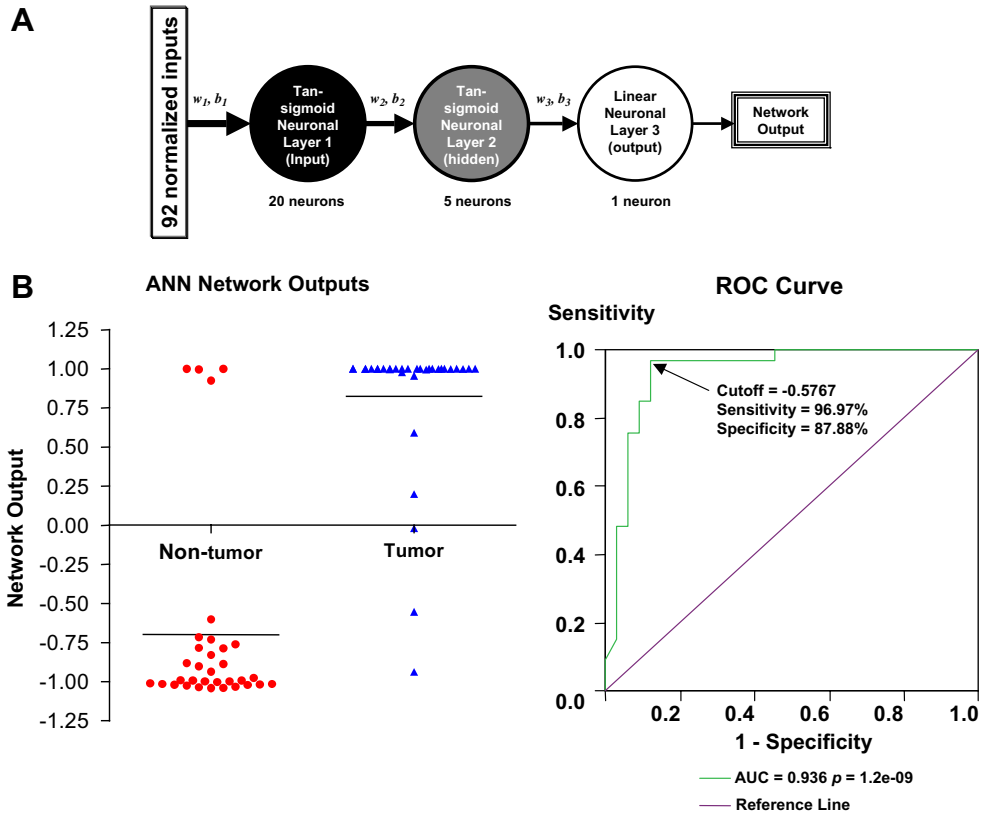

Fig. 1. (A) Topology of the ANN implemented in this study. The network consisted of 92 normalized inputs with range [0, 1]; 20 neurons in the first layer, 5 in the second layer, and 1 in the output layer; Tan-sigmoid transfer function was used in the first two layers, while the output layer was linear with range [−1, 1] in order to generate a linear index of likeliness to be non-tumor or tumor. (B) The network output and performance of ANN constructed in this study. The network output of samples in the validation dataset. The network correctly segregated majority of the samples in both datasets by returning corresponding values for non-tumor (−1) and tumor (1). ROC curve of ANN model. The area under ROC (AUROC) of the model was 0.936, the best sensitivity and specificity were 96.97% and 87.88%, respectively, using cutoff value of −0.5767.

tested and the proportion of true negatives (non-tumor) of all negative samples tested, respectively. Positive predictive value was defined as the proportion of true positive samples from the combined population of true positive and false positive samples.

Results and discussion

Our initial attempt to implement the 2-DE technology as a tool to identify prognostic markers of HCC was successful [17]. In this study, we capitalized from our previous work to expand the sample cohort to 66 HBV-associated HCC patients and applied the 2-DE method to generate liver proteomes from tumor and matched non-tumor tissues. Both the ANN and CART data-mining algorithms were employed to analyze the proteomic profiling data. Our findings indicated that both the procedures provided adequate diagnostic accuracy, i.e., diagnostic sensitivity and specificity for distinguishing between tumor and non-tumor tissues obtained from patients undergoing hepatectomy, a surgical procedure that offers the most effective treatment to patients diagnosed with HCC.

The clinical features of HCC are summarized in Table 1 and the samples were randomly divided into two groups: the model building (training) and blind validation sets. After gel-to-gel matching, normalization, and background subtraction, over 1000 protein spots in the p*I* 4–7 range and relative molecular weight of 10–150 kDa were resolved and revealed by the 2-DE approach. The normalized spot intensities from each proteomic profile ($n = 132$; tumor, 66; non-tumor, 66) were then analyzed by two different algorithms, viz., ANN and CART. The ANN designed in this study showed convergence during training and reached a performance goal of 1.3×10^{-31}. The network outputs of the samples in the validation set are shown in Fig. 1. ANN showed a satisfactory segregation performance in differentiating tumor from non-tumor. Fig. 1B shows the result of ROC analysis based on the validation set, the cutoff value of network output for best classification was −0.5767 with the sensitivity and specificity of 96.97% and 87.88%, respectively. The positive predictive value of the ANN model for HCC was 90.63% and the AUROC was 0.936 with 95% CI of 0.870–1.001.

With the same proteomic dataset, we used the Biomarker Pattern Software to construct a decision classification tree using the CART algorithm, which resulted in five candidate trees (as listed in Table 2). The maximal tree was tree number 1, where it consists of five terminal nodes and lowest cost (best performance). Tree number 2 performed

Table 2
List of candidate classification trees constructed by CART

Tree number	Terminal nodes	Cross-validation cost
1	5	0.273 ± 0.084
2[a]	4	0.273 ± 0.084
3	3	0.364 ± 0.095
4	2	0.333 ± 0.091
5	1	1.000 ± 0.000

[a] The optimal tree with lowest misclassification cost was taken for analysis.

Table 3
The performance of CART on the training set and validation set

	Training set $N = 66$(%)	10-Cross-validation $N = 66$(%)	Validation set $N = 66$(%)
Sensitivity	96.97	90.91	81.82
Specificity	96.97	81.82	78.79
Positive predictive value	96.97	83.33	79.41

equally well as tree number 1, it was chosen as the optimal tree and used for further analyses. The details of the optimal decision tree are shown in Fig. 2. Classification was done recursively from parent to its corresponding child nodes. In this study, the classification tree consisted of three classifier nodes, namely SSP0026, SSP2201, and SSP3102, and they were subsequently identified by MALDI-TOF/MS and MS/MS. SSP0026, SSP2201, and SSP3102 denoted cytochrome b5 (PubMed Accession No.: gi|117809), heat shock 70 kDa protein 8 isoform 2 (PubMed Accession No.: gi|24234686), and cathepsin B (PubMed Accession No.: gi|181178), respectively. These three markers are known to have functional roles in carcinogenesis. Cytochrome b5 functions as a catabolic enzyme of xenobiotics in the liver and it has previous implications in the course of hepatitis C virus-related HCC conditions [19]. Heat shock 70 kDa protein 8 isoform 2 belongs to heat shock protein family, for which family members have shown involvement in the progression of liver cancer [17,20]. Cathepsin B is a cysteine proteinase with an overall up-regulation in various cancers, such as those in colon and lung [21,22]. For every sample, the classification scheme determined the route using the natural log-transformed intensity of the classifier spots in a hierarchical manner and assigned a final class outcome (tumor or non-tumor) in one of the four terminal nodes.

The sensitivities and specificities of CART for the training set and the validation set are summarized in Table 3. The tree correctly identified 96.97% of the samples in the training set. The predicted sensitivities and specificities of the model were 90.91% and 81.82%, respectively. For the validation sample set, CART model correctly identified 27 samples and demonstrated 6 samples to be misclassified as non-tumor, while 26 non-tumor samples were classified accurately with 7 misclassifications as tumor. CART achieved a sensitivity of 81.82%, specificity of 78.79%, and positive predictive value of 79.41%, respectively.

Both the ANN along with logistic regression as well as the CART decision tree model have been reported as the most efficient data mining techniques, particularly with noisy and non-linear datasets commonly seen in clinical

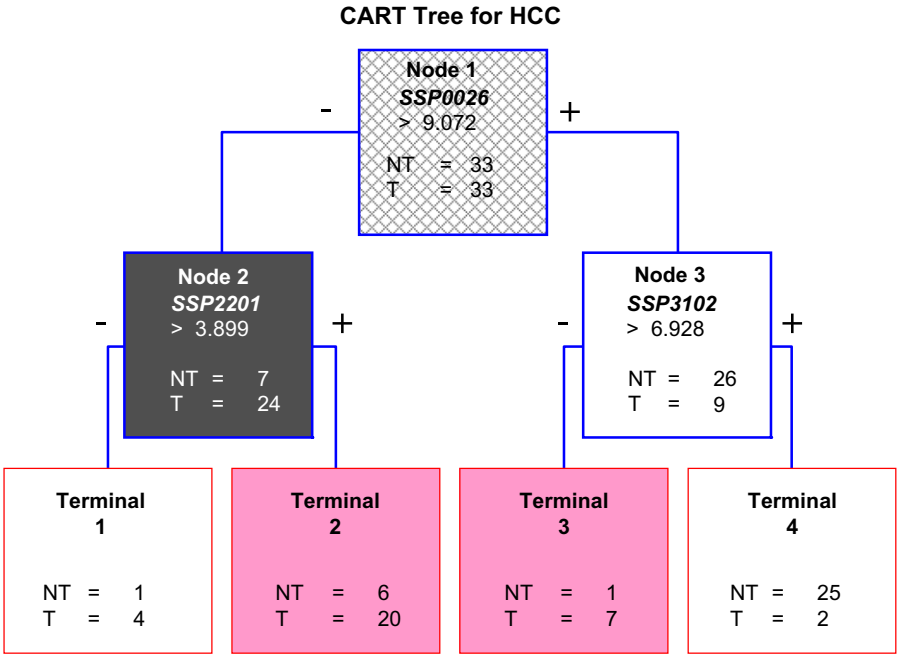

Fig. 2. The optimal classification tree generated by CART. The binary classification tree composed of three classifiers. The decision making process involves the evaluation of if-then rules of each node from top to bottom, which eventually reaches a terminal node with designated class outcome, i.e., tumor (T) or non-tumor (NT).

practice [23,24]. The implementation of ANN and CART in the classification of tumor and non-tumor is one of the first attempts in applying data mining technologies to exploit biological information hidden in the 2-DE based proteomic profiles. In the present study, both the ANN and CART classification models were able to segregate liver samples from tumor to non-tumor with fine accuracies in terms of sensitivities and specificities (ANN: 96.97% and 87.88%; CART: 81.82% and 78.79%). Nevertheless, the discriminative performance of CART was lower than that of ANN in both training and validation tests.

ANN and CART algorithms use different mathematical/computational approaches in the course of inductive learning and result in different ways of classification. ANNs utilized all the neuronal inputs, i.e., the complex proteomic pattern as a marker for the construction of classification model and learn by means of changing its weights and bias, while CART exhaustively searches for a hierarchical set of individual biomarkers and constructs a decision making tree for classification. Both methods offer unique advantages and at the same time suffer from their intrinsic weakness. In this study, ANN seemed to outperform CART in terms of classification, however in terms of marker discoveries, ANN develops classification model in a "black box" manner without a clear logical correlations on how the inputs are used. If one is interested mainly in the potential protein biomarkers for HCC, ANN may not be a suitable approach in contrast to the CART and logistic regression. Furthermore, the training of ANN is relatively complex in terms of implementation and requires a sophisticated computing environment, especially when dealing with a large number of inputs and complex network topologies. On the other hand, CART may outperform ANN in terms of ready implementation and similarity to medical reasoning for the decision-making process. Furthermore, studies also showed that CART could be used as variable selection and data pre-processor for ANN, which might result in higher accuracy and shorter training time [25], indicating that a combination of both techniques is also applicable.

In summary, ANN and CART algorithms were successfully applied for the building of classification model based on the hidden pattern in the proteomic dataset. Cancer biomarker discoveries requiring the application of data mining techniques to proteomic data have recently received much attention. The development of these techniques is an essential part in deciphering the potentials of protein biomarkers or proteomic patterns for clinical practices. Our data suggested that both the ANN and CART models produced good predictive abilities in differentiating between tumor and non-tumor tissues based on their 2-DE proteomic profiles, indicating the effectiveness and promising potentials. Nevertheless, large-scale studies will be necessary to validate these initial results and to determine their clinical usefulness, reproducibility, and accuracies for diagnosis or prognosis of HCC.

Acknowledgments

The work is fully supported by grants (HKU7320/02M; N_HKU718/03) from the Research Grants Council of Hong Kong, Sun Chieh Yeh Research Foundation for Hepatobiliary and Pancreatic and Surgery, and Beijing Municipal Government Foundation for Natural Sciences (No. 7042032).

References

[1] H.B. El-Serag, Hepatocellular carcinoma: an epidemiologic view, J. Clin. Gastroenterol. 35 (2002) S72–S78.
[2] M.P. Waalkes, J. Liu, H. Chen, Y. Xie, W.E. Achanzar, Y.S. Zhou, M.L. Cheng, B.A. Diwan, Estrogen signaling in livers of male mice with hepatocellular carcinoma induced by exposure to arsenic in utero, J. Natl. Cancer Inst. 96 (2004) 466–474.
[3] K. Heinemann, S.N. Willich, L.A. Heinemann, T. DoMinh, M. Mohner, G.E. Heuchert, Occupational exposure and liver cancer in women: results of the Multicentre International Liver Tumour Study (MILTS), Occup. Med. (Lond.) 50 (2000) 422–429.
[4] M.A. Feitelson, B. Sun, N.L. Satiroglu Tufan, J. Liu, J. Pan, Z. Lian, Genetic mechanisms of hepatocarcinogenesis, Oncogene 21 (2002) 2593–2604.
[5] B.W. Wong, J.M. Luk, I.O. Ng, M.Y. Hu, K.D. Liu, S.T. Fan, Identification of liver-intestine cadherin in hepatocellular carcinoma–a potential disease marker, Biochem. Biophys. Res. Commun. 311 (2003) 618–624.
[6] D.B. Kristensen, N. Kawada, K. Imamura, Y. Miyamoto, C. Tateno, S. Seki, T. Kuroki, K. Yoshizato, Proteome analysis of rat hepatic stellate cells, Hepatology 32 (2000) 268–277.
[7] G.S. Yoon, H. Lee, Y. Jung, E. Yu, H.B. Moon, K. Song, I. Lee, Nuclear matrix of calreticulin in hepatocellular carcinoma, Cancer Res. 60 (2000) 1117–1120.
[8] S.Y. Cho, K.S. Park, J.E. Shim, M.S. Kwon, K.H. Joo, W.S. Lee, J. Chang, H. Kim, H.C. Chung, H.O. Kim, Y.K. Paik, An integrated proteome database for two-dimensional electrophoresis data analysis and laboratory information management system, Proteomics 2 (2002) 1104–1113.
[9] L.F. Steel, T.S. Mattu, A. Mehta, H. Hebestreit, R. Dwek, A.A. Evans, W.T. London, T. Block, A proteomic approach for the discovery of early detection markers of hepatocellular carcinoma, Dis. Markers 17 (2001) 179–189.
[10] K.S. Park, S.Y. Cho, H. Kim, Y.K. Paik, Proteomic alterations of the variants of human aldehyde dehydrogenase isozymes correlate with hepatocellular carcinoma, Int. J. Cancer 97 (2002) 261–265.
[11] T.C. Poon, P.J. Johnson, Proteome analysis and its impact on the discovery of serological tumor markers, Clin. Chim. Acta 313 (2001) 231–239.
[12] T.C. Poon, T.T. Yip, A.T. Chan, C. Yip, V. Yip, T.S. Mok, C.C. Lee, T.W. Leung, S.K. Ho, P.J. Johnson, Comprehensive proteomic profiling identifies serum proteomic signatures for detection of hepatocellular carcinoma and its subtypes, Clin. Chem. 49 (2003) 752–760.
[13] T.C. Poon, A.Y. Hui, H.L. Chan, I.L. Ang, S.M. Chow, N. Wong, J.J. Sung, Prediction of liver fibrosis and cirrhosis in chronic hepatitis B infection by serum proteomic fingerprinting: a pilot study, Clin. Chem. 51 (2005) 328–335.
[14] M.T. Hagan, H.B. Demuth, M. Beal, Neural Network Design, PWS Publishing Co., Boston, MA, 1997.
[15] L. Breiman, J.H. Friedman, R.A. Olshen, C.J. Stone, Classification and Regression Trees, Wadsworth Inc, Pacific Glove, 1984.
[16] D. Steinberg, P. Colla, CART—Classification and Regression Trees, Salford Systems, San Diego, 1997.
[17] J.M. Luk, C.T. Lam, A.F. Siu, B.Y. Lam, I.O. Ng, M.Y. Hu, C.M. Che, S.T. Fan, Proteomic profiling of hepatocellular carcinoma in

Chinese cohort reveals heat-shock proteins (Hsp27, Hsp70, GRP78) up-regulation and their associated prognostic values, Proteomics 6 (2006) 1049–1057.

[18] J.M. Luk, Y.C. Su, S.C. Lam, C.K. Lee, M.Y. Hu, Q.Y. He, G.K. Lau, F.W. Wong, S.T. Fan, Proteomic identification of Ku70/Ku80 autoantigen recognized by monoclonal antibody against hepatocellular carcinoma, Proteomics 5 (2005) 1980–1986.

[19] J.F. Blanc, C. Lalanne, C. Plomion, J.M. Schmitter, K. Bathany, J.M. Gion, P. Bioulac-Sage, C. Balabaud, M. Bonneu, J. Rosenbaum, Proteomic analysis of differentially expressed proteins in hepatocellular carcinoma developed in patients with chronic viral hepatitis C, Proteomics 5 (2005) 3778–3789.

[20] M. Takashima, Y. Kuramitsu, Y. Yokoyama, N. Iizuka, T. Toda, I. Sakaida, K. Okita, M. Oka, K. Nakamura, Proteomic profiling of heat shock protein 70 family members as biomarkers for hepatitis C virus-related hepatocellular carcinoma, Proteomics 3 (2003) 2487–2493.

[21] W.J. Kruszewski, R. Rzepko, J. Wojtacki, J. Skokowski, A. Kopacz, K. Jaskiewicz, K. Drucis, Overexpression of cathepsin B correlates with angiogenesis in colon adenocarcinoma, Neoplasma 51 (2004) 38–43.

[22] M.J. Murnane, K. Sheahan, M. Ozdemirli, S. Shuja, Stage-specific increases in cathepsin B messenger RNA content in human colorectal carcinoma, Cancer Res. 51 (1991) 1137–1142.

[23] G. Schwarzer, T. Nagata, D. Mattern, R. Schmelzeisen, M. Schumacher, Comparison of fuzzy inference, logistic regression, and classification trees (CART). Prediction of cervical lymph node metastasis in carcinoma of the tongue, Methods Inf. Med. 42 (2003) 572–577.

[24] W. Dwinnell, Modeling methodology 2: model input selection, PC AI 12 (1998) 32.

[25] W. Dwinnell, Data enhancement-filtering for neural network success, PC AI 14 (2000) 20.